

Solar Magnetograms at 12 μm Using the Celeste Spectrograph

Thomas G. Moran · Donald E. Jennings ·
L. Drake Deming · George H. McCabe · Pedro V. Sada ·
Robert J. Boyle

Received: 13 July 2006 / Accepted: 14 March 2007 /
Published online: 5 May 2007
© Springer 2007

Abstract We present the first solar vector magnetogram constructed from measurements of infra-red Mg I 12.32- μm line spectra. Observations were made at the McMath-Pierce Telescope using the Celeste spectrometer/polarimeter. Zeeman-split Stokes line spectra were fitted with Seares profiles to obtain the magnetic field parameters. Maps of absolute field strength, line-of-sight angle, and azimuth are presented. Analysis shows that the variation in field strength within a spatial resolution element, 2 arcseconds, is greatest in the sunspot penumbra and that this is most likely caused by vertical field strength gradients, rather than horizontal image smearing. Widths of the Zeeman-split σ components, assuming a formation layer thickness of 200 km, indicate that vertical field strength gradients can be as large as 6.5 G/km in a penumbra.

1. Introduction

Magnetic field measurements are crucial for understanding virtually all solar phenomena, such as sunspots, solar flares, coronal loops, coronal mass ejections, waves and oscillations, and coronal heating. Much effort has gone into measuring magnetic fields located

T.G. Moran (✉)
Department of Physics, The Catholic University of America, Washington, DC 20064, USA
e-mail: moran@esa.nascom.nasa.gov

T.G. Moran · D.E. Jennings · L.D. Deming
NASA's Goddard Space Flight Center, Code 693, Greenbelt, MD 20771, USA

G.H. McCabe
CMA Consulting Services, 700 Troy-Schenectady Road, Latham, NY 12110, USA

P.V. Sada
Departamento de Física y Matemáticas, Universidad de Monterrey, Av. I. Morones Prieto 4500 Pte.,
Garza García, LL 66238, Mexico

R.J. Boyle
Department of Physics and Astronomy, Dickinson College, P.O. Box 1773, Carlisle, PA 17013,
USA

from the convection zone through the heliosphere over a wide range of wavelengths. In particular, active regions and sunspots have received considerable attention owing to their association with flares. However, in spite of extensive research in sunspot physics, several important aspects of these structures, such as the magnetic field structure of penumbrae, are still unexplained. Use of infrared (IR) lines in the study of active region fields is especially advantageous, because Zeeman splitting is much greater for IR lines. The 12.32- μm Mg I line is particularly useful for magnetic field studies (Brault and Noyes, 1983; Deming *et al.*, 1989), because its ratio of Zeeman to Doppler broadening is the largest in the solar spectrum. Moreover, it is one of only a few accessible Zeeman sensitive lines formed in the upper photosphere, at the temperature minimum (Chang *et al.*, 1991; Carlsson, Rutten, and Shchukina, 1992), and can provide accurate field strengths closer to the corona than can visible lines. Owing to the magnetic sensitivity of this line, it is often possible to discern multiple field strengths within a spatial resolution element and to estimate the variation in field strength. Polarimetry of such multiple field components might demonstrate that they arise from different horizontal and vertical field structures. Extensive Mg I line modeling studies have demonstrated the sensitivity of these lines to magnetic field characteristics of sunspots and plages (Bruls and Solanki, 1995; Bruls *et al.*, 1995).

Single point magnetic field measurements in the Mg I line made using the McMath-Pierce Fourier Transform Spectrometer at 2.3- and 5-arcsec spatial resolution have revealed the absolute vector field strengths in active regions (Hewagama *et al.*, 1993; Deming *et al.*, 1988) and, coupled with near-IR observations, have yielded absolute field strength variations with height (Moran *et al.*, 2000). The σ components are typically broadened beyond the Doppler and instrumental width, and so line fitting was used to determine the mean field strength. Gaussian profiles were fitted to the π - and σ -line components, and the difference between the sigma profile center wavelengths yielded the mean magnetic field strength.

We have made full-Stokes magnetograms in the Mg I line for the first time using an IR liquid-helium-cooled stigmatic spectrograph, Celeste, coupled to a polarimeter and mounted on the McMath-Pierce Telescope (McCabe *et al.*, 2003). These observations were made at higher spatial coverage and resolution than those of previous Mg I line observations. We present maps made from these measurements using spectral line profile fitting showing absolute field strengths, angle to the line of sight, and azimuth, which reveal field strength and direction in a sunspot and surrounding pores. The implications of field characteristics in the sunspot are explored.

2. Magnetic Field Maps from Mg I IR Observations

2.1. The Celeste IR Polarimetric Spectrograph

The beam from the McMath-Pierce Telescope is collimated, passes through the polarimeter optics, and is focused through the Celeste dewar window onto a cold entrance slit, as shown in Figure 1. The spectrograph achieves nearly diffraction-limited spectral and spatial resolution and background-limited sensitivity. It uses a large echelle grating ($18 \times 33 \text{ cm}^2$) to achieve a dispersion of 0.016 cm^{-1} per pixel and a frequency resolution of 0.04 cm^{-1} on the Mg I 12.32- μm (812-cm^{-1}) line. The detector array is a 128×128 blocked impurity band device with 75- μm pixels, yielding a 1 arcsec per pixel scale, as compared with the 2 arcsec spatial resolution, determined by the telescope diffraction limit at 12.32 μm .

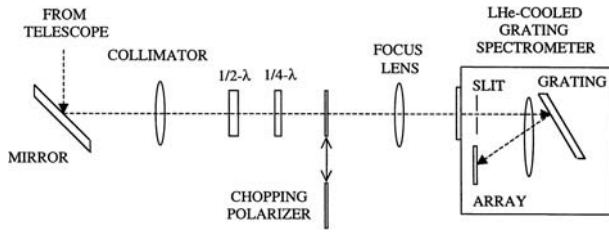


Figure 1 Schematic diagram of the optical path through the 12- μm vector polarimeter. The beam from the telescope formed an image, was collimated, and passed through 1/2- and 1/4-wave plates and a polarization chopper. An image is then formed at the spectrograph entrance slit and the spectrum is dispersed by a grating onto the detector array.

Magnetic field maps were computed from a series of observations taken while stepping the spectrograph slit across the Sun in 2 arcsec steps, at a rate of 5.0 min/step. The image dimensions were determined by the 2.3-arcmin slit length and number of steps. The mapping process, including imaging in the four Stokes parameters, which required observations of 5 min total duration at each step, were performed by using a limb guider, with the entire apparatus under computer control. Stokes measurements in the Mg I line were recorded at each spatial pixel and a data cube (with two spatial dimensions and one spectral dimension) was created for each Stokes parameter. In the polarimeter foreoptics the beam transited a 1/2-wave plate, a 1/4-wave plate, and a chopping linear polarizer. Polarization phase retardations were selected by changing the angles of the two wave plates and the IQUV Stokes parameter differences at each mapping position were obtained by modulating with the chopping polarizer. We used a double-differencing technique to cancel any imbalance between the two polarizer positions. At the first waveplate setting the difference between the two positions of the chopping polarizer gave Q and the second waveplate setting the difference gave $-Q$. The difference between these two measurements yielded Q with cancellation of the background. This cycle was repeated for U and V, and Stokes I was calculated from $I^2 = Q^2 + U^2 + V^2$.

2.2. Mg I Spectral Line Profile Modeling

To determine the mean field strength and variation, we fit the measured Stokes Mg I line spectra to the Seares profiles (Seares, 1913) following the method of Hewagama *et al.* (1993). The Stokes profiles, Φ_I , Φ_V , Φ_Q , and Φ_U , are given by

$$\Phi_I = \frac{1}{2} \phi_\pi \sin^2 \theta + \frac{1}{2} (\phi_b + \phi_r) (1 + \cos^2 \theta), \tag{1}$$

$$\Phi_V = \frac{1}{2} (\phi_b - \phi_r) \cos \theta, \tag{2}$$

$$\Phi_Q = \frac{1}{2} \left(\phi_\pi - \frac{1}{2} (\phi_b + \phi_r) \right) \sin^2 \theta \sin 2\chi, \tag{3}$$

$$\Phi_U = \frac{1}{2} \left(\phi_\pi - \frac{1}{2} (\phi_b + \phi_r) \right) \sin^2 \theta \cos 2\chi, \tag{4}$$

where ϕ_π , ϕ_b , and ϕ_r are modeled as normalized Gaussian functions, θ is the angle between the field direction and the line of sight, and χ is the azimuth. The Stokes I intensity, Φ_I ,

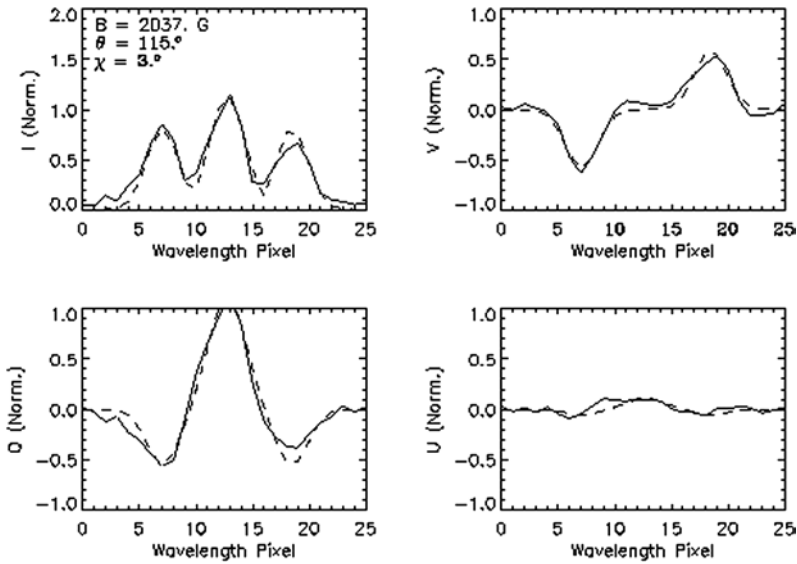


Figure 2 Plots of Stokes I, V, Q, and U Mg I normalized spectral line profiles from the inner penumbra of the sunspot in NOAA region 9433 on 24 April 2001 (solid) and associated Seares profile line fits (dashed). The V, Q, and U values are normalized to I.

is computed from Φ_V , Φ_Q , and Φ_U , by using the relation $\Phi_I^2 = \Phi_V^2 + \Phi_Q^2 + \Phi_U^2$. Spectral line fitting, performed in IDL using the Curvefit.pro gradient-expansion-algorithm routine, determined the central frequencies, widths, and amplitudes of each component, in addition to θ and χ . The amplitudes and widths of the red and blue σ -components are constrained to be equal, and the width of the central π -component Gaussian is fixed to the Celeste instrumental width. The mean magnetic field strength, B_m , is related to the frequency splitting, $\Delta\nu$, by $\Delta\nu = 4.67 \times 10^{-5} B(\text{G}) \text{ cm}^{-1}$. The frequency shift is related to B by $B(\text{G}) = 357\Delta\nu$ (pixels). Magnetic field strength is determined with an accuracy of ~ 70 G for field strengths above 500 G and with an accuracy of ~ 150 G for values below 500 G.

2.3. Mg I Spectral Line Observations

Active region NOAA 9433, at a heliocentric angle of 29° , was observed on 24 April 2001. A flare occurred on the day of the observation and large values of magnetic field strength gradient (5 G/km) were detected in a flaring region pixel through the Mg I observations (Jennings *et al.*, 2002). The eruption occurred in the bipolar region to the east of the sunspot. The data from the flaring region are included in our analysis. We compute the average Stokes parameters over flaring pixels and include the corresponding field parameters in the magnetogram of the region. Stokes I, Q, U, and V profiles from the inner penumbra (2 arcseconds from the umbral boundary) of the sunspot in region 9433 are shown in Figure 2 and the corresponding profiles from the outer penumbra (3 arcseconds from the quiet sun boundary) are shown in Figure 3. The inner penumbral profile shows greater wavelength splitting and field strength variation. The field strengths measured were 2037 and 1187 G, respectively. The σ components were fully resolved in the inner penumbra and partially resolved in the outer penumbra.

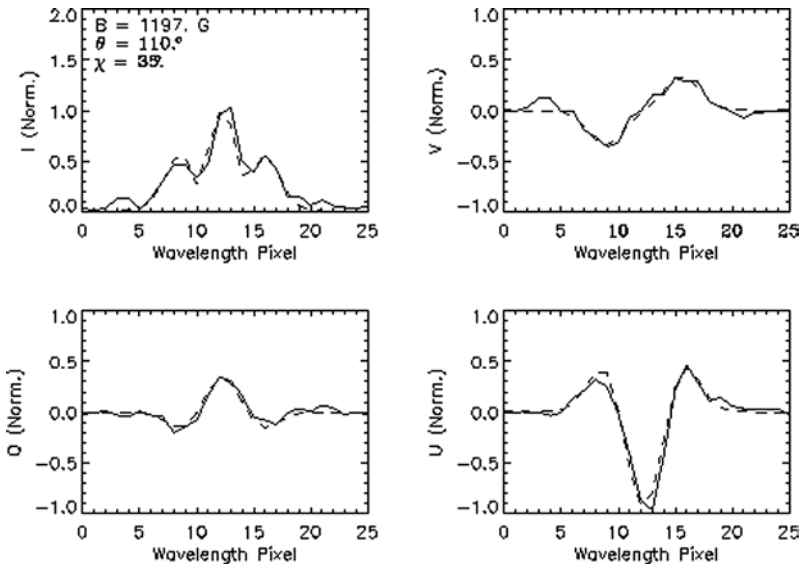


Figure 3 Plots of Stokes I, V, Q, and U Mg I normalized spectral line profiles from the outer penumbra of the sunspot in NOAA region 9433 on 24 April 2001 (solid) and associated Seares profile line fits (dashed). The V, Q, and U values are normalized to I.

2.4. Magnetic Field Maps

Shown in Figure 4 are maps of the NOAA region 9433 12- μm continuum (a), the field strength determined from the Mg I line (b), the line-of-sight angle θ (c), and the azimuth χ (d). Continuum intensity is computed by integrating emission over 20 off-line wavelength pixels on the Celeste detector array. A flare occurred in the bipolar region to the east of the spot, visible in Figure 4b. Large values of magnetic field strength gradient (5 G/km) were detected in a flaring region pixel through the Mg I observations (Jennings *et al.*, 2002). The data from the flaring region are included in our analysis. We compute the average Stokes parameters over flaring pixels and include the corresponding field parameters in the magnetogram of the region.

Although intensity errors from variable sky transmission resulted in a limit on detectable contrast, the sunspot and surrounding pores are clearly visible in the continuum image in Figure 4a. Black and white values in Figure 4b indicate positive and negative polarity, respectively. Plots of the field strength, line-of-sight angle, and azimuth along a N–S chord in the penumbra indicated in Figure 4b are shown in Figure 5. As expected, the field strength is greatest in the inner penumbra and decreases from a maximum of 2300 G at the umbral boundary to a minimum of 900 G at the quiet sun boundary, approximately consistent with past measurements of penumbral field strengths in the Mg I line (Deming *et al.*, 1988; Hewagama *et al.*, 1993). Field strength varies approximately as r^{-1} , consistent with a radial field configuration and with previous Mg I sunspot observations. If the field is radially directed, the area filled will be proportional to r , and since magnetic flux is conserved, the field strength would fall as r^{-1} . The mean field is not radially directed, but some components of it such as filamentary fields might be. It is well known from magnetic field measurements made in sunspots using visible observations that narrow radially aligned

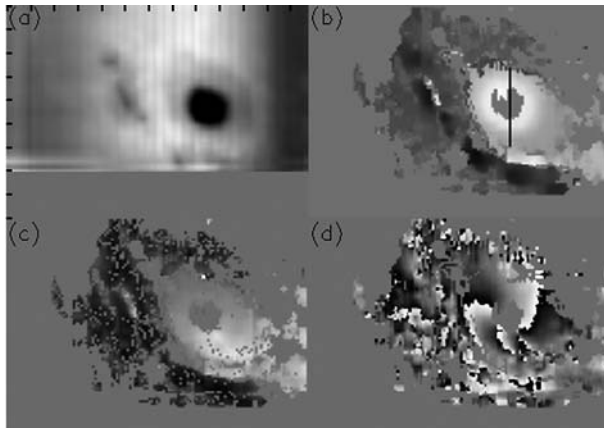
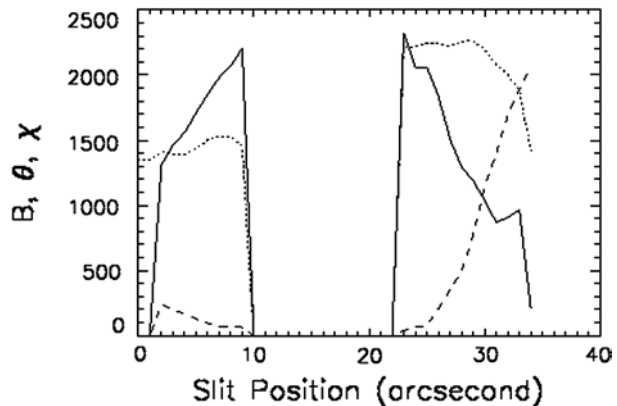


Figure 4 Maps of NOAA region 9433 on 24 April 2001 showing (a) 12- μm continuum intensity, (b) magnetic field strength (with black and white indicating negative and positive polarity, respectively), (c) angle between the field direction and the line of sight, θ , and (d) azimuth χ . The magnetic field strength map shows no information in the umbra since the Mg I line is not in emission there. Negative- and positive-polarity field strength limits are -2400 and 2500 G, respectively, θ varies between 40° and 170° , and χ varies between 0 and 90° . The frames are 128 arcseconds \times 90 arcseconds in size and oriented N–S in Earth-based coordinates. The image scale is indicated by the tick marks on Figure 4a, spaced at 10 arcseconds. The spatial resolution is 2 arcseconds, twice the pixel size of 1 arcsecond. Intensity values were not computed for the lower 20 arcseconds of the frame, shown in Figure 4a, owing to low signal-to-noise ratios. The magnetic field strength and angle values measured from north to south along the chord indicated in Figure 4b are plotted in Figure 5.

Figure 5 Plots of the magnetic field strength (solid), angle to the line of sight, θ (dotted) (degrees $\times 15$) and azimuth χ , (dashed) (degrees $\times 20$) from NOAA active region AR9433 on 24 April 2001, through a N–S chord across the sunspot. The angle θ is 0° in the direction away the observer, so the angle from a ray directed at the Earth equals $180^\circ - \theta$. The pixel size is 1 arcsecond and the spatial resolution is 2 arcseconds.



structures known as fibrils have radially directed fields (e.g., Lites and Skumanich, 1990; Lites *et al.*, 1993).

The Mg I line emits in the penumbra and just inside the umbra, but not in the umbral core, owing to its low temperature. The emission inside the boundary may arise from fibrils radiating in the Mg I line, which extend slightly into the continuum umbra. This scenario is supported by the presence of filamentary structures extending into the umbra from the northern boundary as seen in Figure 4b. These two fibrils form a fork-like structure east of and aligned along the indicated chord through the umbra. They emit in the Mg I line, but not in the 12- μm continua, which is formed 200 km below the Mg I line emission layer, sug-

gesting they lie over the umbra. Furthermore, the azimuth is constant along these structures, consistent with a radial fibril field. Finally, their thickness at the furthest extent into the umbra is no more than 2 arcseconds, equal to the spatial resolution, indicating the objects are 1 arcsecond or less in width, also consistent with fibrils.

The map of the angle to the line of sight, θ , demonstrates the outward direction of field lines in the sunspot. Field lines from penumbral positions closest to Sun center are most inclined along the line of sight, with minimum values of 3° from the Earth–Sun line. On the boundary on the opposite side of the spot, angles are a maximum of 80° from the line of sight. Along a chord through Sun center, the penumbral boundary field angular span from the surface vertical is 100° , so field lines at the boundary are oriented 40° from the surface horizontal, as compared with angles of $\sim 20^\circ$ measured at penumbral boundaries with visible observations (Lites and Skumanich, 1990). Lites and Skumanich (1990) point out that the field may have multiple components, as measured in several visible studies (Degenhardt and Wiehr, 1991; Stanchfield, Thomas, and Lites, 1997). Thus, the angle measured might not represent a single field. The difference between the IR Mg I and visible measurements may result from a different weighting of field components.

The map of the azimuth χ shows significant variations in both the pores and the spot. Since the spatial resolution is 2 arcseconds, the values computed in pores are averages over small-scale variations and do not provide detail on field structure. Field lines between the spot and pore region are directed along a line separating the two areas, indicating magnetic shear. Within the penumbra and in the area adjacent to the spot, there are kinks in the χ contours that suggest a spiral structure. However, the active region is complicated and the spot field configurations are affected by nearby pores, so it is not clear that the penumbral field has a spiral component.

3. Field Variation in Sunspot Penumbra

Horizontal field variations over the flaring region were discussed in Jennings *et al.* (2002). From our line-fitting analysis, we may also compute the variation in penumbral field strength in the Mg I formation layer within a resolution element through a measurement of the spectral line σ -component width. The inner and outer penumbral spectral lines plotted in Figures 2 and 3 for σ -component widths correspond to 1 430 and 1 030 G, respectively. The true σ -component and instrumental widths, Δv_t and Δv_i , add in quadrature to yield the measured width, $\Delta v_m^2 : \Delta v_m^2 = \Delta v_t^2 + \Delta v_i^2$. True widths were computed for both line spectra by using this relation. The resulting field strength variation within a resolution element is equal to 1 300 and 700 G for the inner and outer penumbral spectra, respectively.

The variation in field strength resulting from finite spatial resolution is determined by the field strength horizontal gradient and the spatial resolution. The maximum field strength gradient along the chord shown in Figure 4b is equal to 200 G/pixel. Since this gradient is measured over 7 pixels and the spatial resolution is 2 pixels, it represents the true field gradient. Thus, the field strength variation resulting from finite spatial resolution equals 400 G. Therefore, the measured variations in penumbral field strength of 1 300 and 700 G do not result from finite spatial resolution.

One possible explanation for the large field strength variation is vertical gradients in field strength within the Mg I formation layer. Detailed modeling of Mg I line formation suggests that the layer is approximately 200 km thick (Carlsson, Rutten, and Shchukina, 1992). This is consistent with annular solar eclipse measurements of Mg I line emission at the limb (Deming *et al.*, 1998) but is less than the 600-km thickness measured through total solar

eclipse observations (Deming *et al.*, 1992). The difference between the two observations may be caused by spatial variations in the solar atmosphere. For the purpose of calculating field gradients, we will use a thickness of 200 km, consistent with Mg I quiet sun line-formation theory (Carlsson, Rutten, and Shchukina, 1992). If we assume that the formation thickness in the spot equals that in the quiet sun, variations of 1 300 and 700 G over 200 km in height then correspond to field strength gradients of 6.5 and 3.5 G/km in the inner and outer penumbra, respectively. However, the formation thicknesses within the spot may be greater than 200 km. If we assume a maximum formation thickness of 600 km, the inferred gradients are 2.2 and 1.2 G/km, for the inner and outer penumbra, respectively. Note that the gradient in the spot center is larger than in the penumbra, but it cannot be measured using Mg I observations. Large Mg I σ -component widths have previously been attributed to vertical field strength variations in a study that determined that the gradient exceeded 1 G/km (Deming *et al.*, 1988), in contrast to magnetostatic sunspot models (Pizzo, 1986; Osherovich, 1984). These gradients determined in our study are larger than those computed from simultaneous measurements of penumbral field strength at two heights from observations at 12.32 and 1.5 μm (2 G/km; Moran *et al.*, 2000) and are larger than those computed from near-simultaneous measurements of deep photospheric and chromospheric penumbral field strengths (0 to 0.5 G/km; Leka and Metcalf, 2003). However, the vertical field strength gradient in the Mg I formation layer is most likely greater than the mean gradient between lower and upper photosphere since the field diverges nonlinearly. Sunspot fields must diverge rapidly at some height in the chromosphere or below, since field strengths there are measured to be at least 30% weaker on average than underlying active region photospheric values (Leka and Metcalf, 2003). The field apparently spreads out widely in the Mg I formation layer, explaining the large σ -component widths.

4. Magneto-Optical Effects on Mg I Line Polarization

The polarization state of light propagating through magnetized plasma can be altered through coupling of the wave electric field vector and the gyrating electrons. Consider a linearly polarized wave traveling along the field direction. The polarization vector may be expressed as sum of right- and left-hand circularly polarized components. The electrons couple to the right-hand polarized component, altering the corresponding index of refraction and phase speed. This causes the right- and left-hand components to travel at different speeds, resulting in rotation of the polarization vector as the light traverses the plasma. The rotation angle, $\Delta\chi$, is given by (Krall and Trivelpiece, 1973)

$$\Delta\chi = 2.34 \times 10^{-4} f^{-2} \int n_e B \cos\theta \, dz, \quad (5)$$

where n_e (cm^{-3}) is the electron density, f (s^{-1}) is the wave frequency, B (G) is the field strength, and $\Delta\chi$ is given in radians. The integral extends from the emitting region to the observer. If we assume constant field strength and line-of-sight angle, the rotation angle is given by

$$\Delta\chi = 2.34 \times 10^{-4} f^{-2} B \cos\theta \int n_e \, dz. \quad (6)$$

For the Mg I line emission and a mean penumbral field strength component of 1 000 G along the field,

$$\Delta\chi = 4.1 \times 10^{-28} \int n_e \, dz. \quad (7)$$

The integral of the density over the emitting region may be estimated from detailed line-emission models and from solar eclipse measurements. We take the emitting layer thickness to be 200 km, or 2×10^7 cm. The maximum mean electron density in the layer, determined from detailed line modeling, is 4×10^{11} cm^{-3} (Chang and Schoenfeld, 1991). If the density were higher than this value, the line would be significantly Stark-shifted from its observed frequency owing to collisional electric fields. The integral in Equation (7) can then be estimated at 6×10^{18} cm^{-2} , and the rotation angle $\Delta\chi$ is equal to 2.4×10^{-9} radians, or 1.4×10^{-7} degrees. Thus, the angular shift from Faraday rotation is negligible, even if we are underestimating the density and layer thickness by a factor of 2, and the computed azimuth map shows the true field direction in the plane of the sky.

5. Discussion

We have shown that the Celeste IR spectrograph/polarimeter can provide detailed active region vector magnetograms, including absolute field strengths, through measurements of Mg I 12- μm line spectra. These magnetograms are the first constructed from measurements at 12 μm . Through these observations, the magnetic field structures of sunspots, pores, and plage at the Mg I formation height, the upper photosphere can be investigated. These measurements yield unique field information in this region, which is particularly important for understanding the coupling of fields and plasma in the corona. The large field strength gradient of 6.5 to 3.2 G/km found in sunspot penumbra under the assumption of an Mg I formation thicknesses of 200 to 600 km is too large to be explained by horizontal variations in field strength and image smearing and may result from the fanning out of field lines below the chromosphere.

Acknowledgements This work was supported in part by a grant from the NASA Solar and Heliospheric Physics program. The observations for this study were carried out with the help of Claude Plymate at the McMath-Pierce Telescope at the National Solar Observatory at Kitt Peak, Arizona. Many comments made by the referee have improved this manuscript.

References

- Brault, J.W., Noyes, R.W.: 1983, *Astrophys. J.* **269**, L61.
 Bruls, J.H.M.J., Solanki, S.K.: 1995, *Astron. Astrophys.* **293**, 240.
 Bruls, J.H.M.J., Solanki, S.K., Rutten, R.J., Carlsson, M.: 1995, *Astron. Astrophys.* **293**, 225.
 Carlsson, M., Rutten, R.J., Shchukina, N.G.: 1992, *Astron. Astrophys.* **253**, 567.
 Chang, E., Schoenfeld, W.: 1991, *Astrophys. J.* **383**, 450.
 Chang, E.S., Avrett, E.H., Mauas, P.J., Noyes, R.W., Loeser, R.: 1991, *Astrophys. J.* **379**, L79.
 Degenhardt, D., Wiehr, E.: 1991, *Astron. Astrophys.* **252**, 821.
 Deming, D., Boyle, R.J., Jennings, D.E., Wiedemann, G.: 1988, *Astrophys. J.* **333**, 978.
 Deming, D., Boyle, R.J., Jennings, D.E., Wiedemann, G.: 1989, *Astrophys. J.* **338**, 1193.
 Deming, D., Jennings, D., McCabe, G., Noyes, R., Weideman, G., Espenak, F.: 1992, *Astrophys. J.* **386**, L53.
 Deming, D., Jennings, D.E., McCabe, G., Moran, T., Loewenstein, R.: 1998, *Solar Phys.* **182**, 283.
 Hewagama, T., Deming, D., Jennings, D.E., Osheroich, V., Wiedemann, G., Zipoy, D., Mickey, D.L., Garcia, H.: 1993, *Astrophys. J. Suppl.* **86**, 313.
 Jennings, D.E., Deming, D., McCabe, G., Sada, P.V., Moran, T.: 2002, *Astrophys. J.* **568**, 1043.
 Krall, N., Trivelpiece, A.: 1973, *Principles of Plasma Physics*. McGraw-Hill, New York, 186.
 Leka, K.D., Metcalf, T.: 2003, *Solar Phys.* **212**, 361.
 Lites, B., Skumanich, A.: 1990, *Astrophys. J.* **348**, 747.
 Lites, B., Elmore, D., Seagraves, D., Skumanich, A.: 1993, *Astrophys. J.* **418**, 928.
 McCabe, G.H., Jennings, D.E., Deming, D., Sada, P., Moran, T.: 2003, *Proc. SPIE* **4843**, 39.
 Moran, T., Deming, D., Jennings, D.E., McCabe, G.: 2000, *Astrophys. J.* **533**, 1035.

Osherovich, V.: 1984, *Solar Phys.* **90**, 31.

Pizzo, V.: 1986, *Astrophys. J.* **302**, 785.

Seares, F.H.: 1913, *Astrophys. J.* **38**, 99.

Stanchfield, D., Thomas, J., Lites, B.: 1997, *Astrophys. J.* **477**, 485.